Crystal Structure of Rabbit Phosphoglucose Isomerase Complexed with Its Substrate D-Fructose 6-Phosphate‡

Ji Hyun Lee, Kathy Z. Chang, Vishal Patel, and Constance J. Jeffery*

Laboratory for Molecular Biology, MC567, Department of Biology, University of Illinois at Chicago, Chicago, Illinois 60607

Received December 22, 2000; Revised Manuscript Received May 11, 2001

ABSTRACT: Phosphoglucose isomerase (PGI, EC 5.3.1.9) catalyzes the interconversion of D-glucose 6-phosphate (G6P) and D-fructose 6-phosphate (F6P) and plays important roles in glycolysis and gluconeogenesis. Biochemical characterization of the enzyme has led to a proposed multistep catalytic mechanism. First, the enzyme catalyzes ring opening to yield the open chain form of the substrate. Then isomerization proceeds via proton transfer between C2 and C1 of a *cis*-enediol(ate) intermediate to yield the open chain form of the product. Catalysis proceeds in both the G6P to F6P and F6P to G6P directions, so both G6P and F6P are substrates. X-ray crystal structure analysis of rabbit and bacterial PGI has previously identified the location of the enzyme active site, and a recent crystal structure of rabbit PGI identified Glu357 as a candidate functional group for transferring the proton. However, it was not clear which active site amino acid residues catalyze the ring opening step. In this paper, we report the X-ray crystal structure of rabbit PGI complexed with the cyclic form of its substrate, D-fructose 6-phosphate, at 2.1 Å resolution. The location of the substrate relative to the side chains of His388 suggest that His388 promotes ring opening by protonating the ring oxygen. Glu216 helps to position His388, and a water molecule that is held in position by Lys518 and Thr214 accepts a proton from the hydroxyl group at C2. Comparison to a structure of rabbit PGI with 5PAA bound indicates that ring opening is followed by loss of the protonated water molecule and conformational changes in the substrate and the protein so that a helix containing amino acids 513−520 moves in toward the substrate to form additional hydrogen bonds with the substrate.

Phosphoglucose isomerase (PGI,[1] EC 5.3.1.9) catalyzes the interconversion of D-glucose 6-phosphate (G6P) and D-fructose 6-phosphate (F6P). This reaction is the second step in glycolysis and is also important in gluconeogenesis and the glycosylation of proteins.

Although PGI is a cytosolic glycolytic enzyme, its DNA sequence also encodes three extracellular cytokines and growth factors: neuroleukin (NL) (*1*, *2*), autocrine motility factor (AMF) (*3*, *4*), and differentiation and maturation mediator (DMM) (*5*). Neuroleukin stimulates antibody secretion by mononuclear blood cells and fosters the survival of embryonic spinal neurons in vitro (*6*, *7*). AMF is being studied for a possible role in cancer metastasis because it promotes an increase in tumor cell motility in vitro. DMM causes differentiation of human myelogenous leukemia cells (*8*) and a human promyelocytic cell line (HL-60 cells) (9, *10*) to terminal monocytic cells. While it is not clear if there is any difference between PGI and the three cytokines in vivo, such as a posttranslational modification, it has been demonstrated that purified PGI causes the same changes in tumor cell motility and leukemia cell differentiation as AMF or DMM.

PGI enzymatic activity was first described by Lohmann in 1933 (*11*). Subsequent studies of PGI by several laboratories resulted in extensive biochemical characterization of the enzyme. A proposed multistep catalytic mechanism involves general acid/base catalysis with proton transfer (*12*−*15*). The reaction proceeds readily in both the forward (G6P to F6P) and reverse (F6P to G6P) directions in vitro. Since G6P and F6P exist predominantly in their cyclic forms in solution (*16*), it is believed that the cyclic form of the substrate binds to the enzyme, and active site amino acid residues catalyze opening of the hexose ring to produce the open chain form of the substrate (*17*). In the forward reaction, abstraction of a proton from C2 then yields the proposed a 1,2-*cis*-enediol(ate) intermediate. Donation of a proton back to the intermediate on C1 results in formation of the open chain form of F6P.

Several previously reported PGI crystal structures contained competitive inhibitors of isomerase catalytic activity bound in the active site. Crystal structures of rabbit PGI contained 6-phospho-D-gluconate (6PGA) (*18*) or 5-phospho-D-arabinonate (5PAA) (*19*). *Bacillus stearothermophilus* PGI structures contained 5PAA or *N*-(bromoacetyl)ethanolamine phosphate in the active site (*20*). *N*-(bromoacetyl)ethanolamine phosphate is a linear molecule that forms a covalent bond with a histidine in the PGI active site. 6PGA and 5PAA

‡ Coordinates for the structure of phosphoglucose isomerase complexed with the substrate fructose 6-phosphate are deposited in the Protein Data Bank with the ID code 1HOX.

* To whom correspondence should be addressed. E-mail: cjeffery@uic.edu. Tel: 312-996-3168. Fax: 312-413-2691.

[1] Abbreviations: PGI, phosphoglucose isomerase; PDB, Protein Data Bank; AMF, autocrine motility factor; NL, neuroleukin; DMM, differentiation and maturation mediator; 6PGA, 6-phospho-D-gluconate; 5PAA, 5-phospho-D-arabinonate; G6P, D-glucose 6-phosphate; F6P, D-fructose 6-phosphate.

10.1021/bi002916o CCC: $20.00
Published on Web 06/08/2001

are similar to the open chain form of the substrate, and 5PAA resembles the *cis*-enediol(ate) intermediate. In fact, the rabbit PGI/5PAA complex crystal structure identified Glu357 as the amino acid residue that transfers a proton during the isomerization step of the catalytic mechanism. However, none of the crystal structures identified the mechanism by which the enzyme catalyzes the ring opening step of the reaction. To identify the active site amino acid residues involved in the ring opening step of catalysis, it would be helpful to have a structure of PGI with the cyclic form of a competitive inhibitor or substrate bound in the active site. We report herein the X-ray crystal structure of rabbit PGI with the cyclic form of D-fructose 6-phosphate bound in the active site. The PGI/F6P complex crystal structure was determined at 2.1 Å resolution.

EXPERIMENTAL PROCEDURES

Cocrystallization of PGI with G6P. Rabbit skeletal muscle PGI was purchased from Sigma Chemical Co. The protein was desalted by ion-exchange chromatography and concentrated as described previously (*18*). Crystals were grown by the hanging drop vapor diffusion method at room temperature. The hanging drops contained an equal mixture of protein solution [18−20 mg/mL PGI, 5 mM D-glucose 6-phosphate, 10 mM imidazole (pH 7.5), and 50 mM KCl] and reservoir solution [14.5% PEG 8000, 250 mM magnesium acetate, and 100 mM sodium cacodylate (pH 6.5)]. The drops were allowed to equilibrate with 1 mL of reservoir solution. The crystals grew as colorless hexagonal rods.

Data Collection. A diffraction data set from a single crystal of PGI complexed with F6P was collected at the APS beamline 14C (BioCARS) at Argonne National Laboratories using monochromatic X-rays. The crystal was approximately $0.2 \times 0.3 \times 0.4$ mm^3 in size and had the symmetry of the orthorhombic space group $C222_1$ ($a = 82.44$ Å, $b = 119.43$ Å, $c = 272.14$ Å). Immediately before data collection, the crystal was soaked briefly in a stabilization solution containing 16% PEG 8000, 250 mM magnesium acetate, 100 mM sodium cacodylate (pH 6.5), 5 mM glucose 6-phosphate, and 20% glycerol, and the crystal was flash frozen at −180 °C. The data set was processed with the programs DENZO and SCALEPACK (*21*).

Structure Refinement. Refinement consisted of alternating rounds of computational refinement using the CNS program package (*22*) and manual fitting of the model to electron density maps using the program O (*23*). The initial model for refinement was a previously reported rabbit PGI structure [PDB entry 1DQR (*18*)] from which all of the water molecules and the inhibitor molecule were removed. Ten percent of the data set was set aside to compute R_{free} (*24*). Simulated annealing was used to remove model bias. Data between 30 and 2.1 Å resolution were used in positional and *B* factor refinement with a bulk solvent correction applied. During each round of refinement, the CNS program package was used to suggest potential water molecules using electron density maps with coefficients of $|F_o - F_c|$. Water molecules were then added to the model on the basis of those electron density maps, geometry, and refined *B* factors. During the final rounds of refinement, a D-fructose 6-phosphate molecule was built into each of the two active sites in the PGI molecule. Stereochemistry of the model was checked with the programs CNS and PROCHECK (*25*). The final *R* factor is 19.3 for all data from 30 to 2.1 Å resolution with a free *R* factor of 23.4 (Table 1).

Table 1: Statistics for Data Collection and Refinement[a]

data collection	
space group	$C222_1$
cell dimensions (Å)	
a	82.44
b	119.43
c	272.14
temperature (°C)	−180
resolution range (Å)	30−2.1 (2.18−2.10)
observed reflections	
total	315852 (31147)
unique	77413 (7640)
completeness (%)	98.6 (98.3)
redundancy	4.08 (4.08)
R_{sym} (% on I)	0.049 (0.346)
refinement	
resolution range (Å)	30−2.1
R factor (%)	19.3
R_{free} (%)	23.4
ordered water molecules	868
rmsd from ideal geometry	
bond lengths (Å)	0.007
bond angles (deg)	1.290
average *B* factor (Å^2)	35.1

[a] $R_{sym} = \sum|I_i - \langle I\rangle|/\sum I_i$. *R* factor $= \sum|F_o - F_c|/\sum F_o$. R_{free} is the equivalent of *R* factor, but it is calculated for a 10% randomly chosen set of reflections that were omitted from the refinement process. The numbers in parentheses refer to the last shell of data.

RESULTS AND DISCUSSION

The crystal structure of PGI with a bound substrate, fructose 6-phosphate, has been solved at 2.1 Å resolution by X-ray crystallography. The asymmetric unit contains one homodimer of PGI, and the dimer is similar to the two other reported structures of rabbit PGI (*18*, *19*). The root-mean-square deviation in α carbon positions is 0.53 Å when compared to the PGI/6PGA structure and 0.52 Å when compared to the PGI/PAA structure. Each subunit contains two α/β sandwich domains and a C-terminal region that extends around the other subunit in the dimer. Each subunit is made up of 557 amino acid residues, but the two C-terminal amino acid residues are disordered and have not been included in the final model. The two subunits are similar to each other, with a root-mean-square deviation in α carbon positions of only 0.37 Å. The final model also includes 868 water molecules per asymmetric unit.

Substrate Binding. A simulated annealing omit map calculated with the coefficients $|2F_o - F_c|$ and contoured at 1.5σ contains electron density for a bound fructose 6-phosphate molecule in each substrate binding pocket (Figure 1). These binding sites correspond to the binding sites for 5PAA and 6PGA in the PGI/5PAA and PGI/6PGA crystal structures. Each binding pocket is composed mainly of amino acids from one subunit, with a few amino acid residues, including His388, contributed from the other subunit in the dimer.

In each active site, the shape of the electron density for the ligand is clearly pentagonal in shape, which is consistent with the ligand being D-fructose 6-phosphate, and not hexagonal, which would be consistent with a bound D-glucose 6-phosphate molecule. Attempts to fit D-glucose 6-phosphate

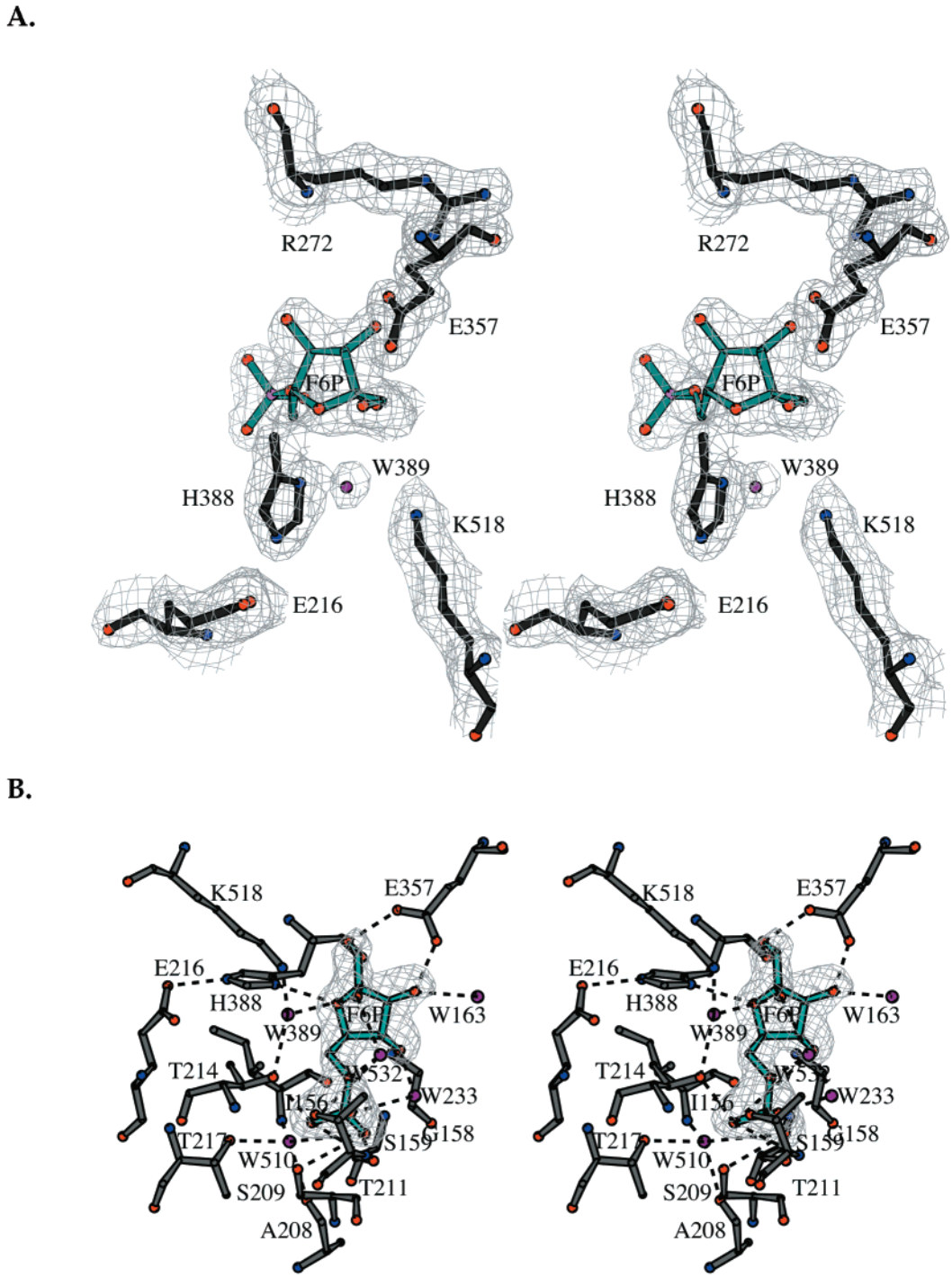

FIGURE 1: PGI active site with bound F6P. (A) Electron density map of the active site. Part of an electron density map surrounding the bound F6P substrate and active site amino acid residues His388, Lys518, Arg272, Glu216, Glu357, and water 389 is shown in stereo. The electron density map (gray) was calculated with coefficients of $|2F_o - F_c|$ and shown with a 1.5σ contour level. Panels A and B of this figure and Figures 2 and 3A were made using the program BOBSCRIPT (*31*). (B) Hydrogen bond interactions with the substrate. A ball-and-stick diagram of F6P is shown (green) relative to several active site residues, including His388, Lys518, and Thr214 (dark gray), and ordered water molecules (purple). Hydrogen-bonding interactions are indicated by dashed lines. A simulated annealing omit electron density map (gray) was calculated by leaving out the F6P. The electron density map is shown with a 1.5σ contour level.

into the electron density maps were not successful. Apparently, the substrate added to the cocrystalization solutions, G6P, was converted to product, F6P, which is the substrate for the reverse reaction. Bulges in the electron density at three of the vertices of the pentagon correspond to the sugar hydroxyl groups. The lack of a bulge at one vertex indicates the position of the ring oxygen, which also aided in the orientation of the ring in the active site. The shape of the electron density corresponding to the substrate C1 and C2 hydroxyl groups indicates that the bound substrate is the β anomer of D-fructose 6-phosphate. The side chain of Glu357 forms hydrogen bonds with the C1 and C3 hydroxyl groups and appears to play a role in specificity for the β anomer.

F6P is oriented in each active site so that the phosphate group forms hydrogen bonds with the side chains and backbone amide and carbonyl groups from several active

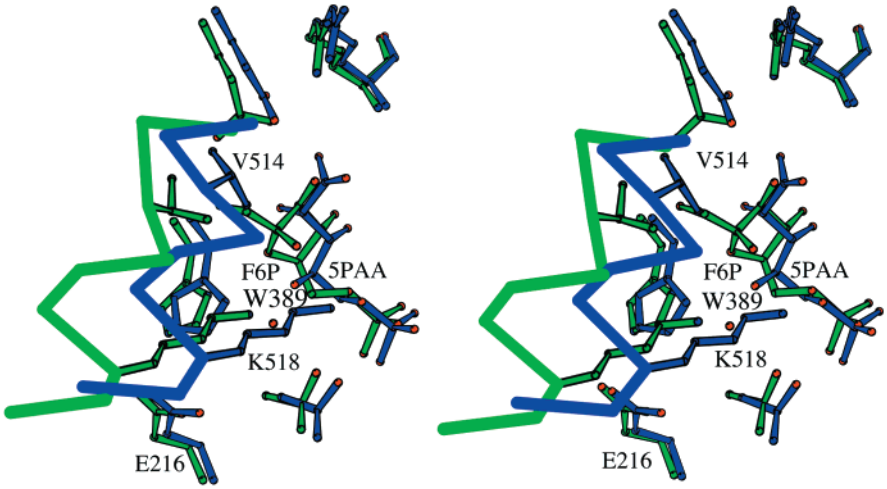

FIGURE 2: Superposition of the active sites of the rabbit PGI/5PAA complex (blue) and the PGI/F6P complex (green). A significant difference in the interaction of the ligands with PGI is that the C1 hydroxyl group of 5PAA is located farther from Val514 and closer to Arg272. The helix containing amino acids 513−520 (shown as an α carbon trace) moves in toward the substrate. Without the conformational change in the substrate, Val514 would be too close to the substrate C1 hydroxyl group to allow movement of the helix. Water 389 is absent from the PGI/5PAA structure, and instead Lys518 interacts directly with the substrate.

site amino acid residues and with ordered water molecules. The interactions between F6P and the enzyme are similar to the interactions reported previously between rabbit PGI and the competitive inhibitors 6PGA and 5PAA (Figure 1B) (*18*, *19*). The phosphate group of F6P forms hydrogen bonds with the side chains of Thr214, Ser209, Ser159, and Thr211 and the backbone amide groups from residues Lys210 and Thr211. Water molecules 510 and 233 also interact with the F6P phosphate group. In addition, water 510 forms hydrogen bonds with the side chain of Thr217, the carbonyl oxygen of Ala208, and the amide group of Ile156.

The hydroxyl groups at the C3 and C4 positions of F6P also form interactions with the enzyme. OH3 forms hydrogen bonds to the side chain of Glu357 and two ordered water molecules, water 163 and water 384. Water 163 forms hydrogen bonds with the backbone amide nitrogen and side chain of Arg272 and the side chain of Glu357. Water 384 forms a hydrogen bond with water 185 and water 532. (Water 532 also makes hydrogen bonds with the substrate O2 hydroxyl group, O6, and the phosphoryl group.) The hydroxyl group on OH4 forms hydrogen bonds with water 233 and the backbone nitrogen of Gly158.

A comparison of the active sites of the PGI/F6P and PGI/5PAA complex structures revealed that, while most of the atoms of the ligand are in similar positions relative to the protein, there is a significant difference in the positions of C1 and OH1 (Figure 2). There is a rotation of approximately 140° around the substrate C3−C4 bond (corresponding to the C2−C3 bond in the 5PAA inhibitor). As a result, the C1 and OH1 of 5PAA are located on the other side of Asp357, nearer to the side chain of Arg272.

A comparison of the protein conformation in the rabbit PGI/5PAA, PGI/6PGA, and PGI/F6P complex structures reveals that the PGI/F6P structure is still in the "open" conformation as was seen in the structure of the PGI/6PGA complex. PGI with the cyclic form of F6P bound cannot shift to the closed conformation because movement of the helix containing residues 513−520 toward the substrate would result in steric clash between Val514 and both the substrate C1 and the hydroxyl group on C1. After superposition of the PGI/5PAA and the PGI/F6P structures with the program O (*23*) using α carbons from residues 100−400, the distance between the Val514 CG1 and the F6P C1 is only 1.2 Å and the distance between the Val514 CG1 and the F6P O1 is 1.7 Å (Figure 2). Also important, in the closed conformation, Lys518 interacts directly with the substrate OH5 and O6 (corresponding to OH4 and O5 in the PGI/5PAA complex). In this new position, Lys518 probably helps to position the substrate correctly for the subsequent isomerization step. If the helix moved upon substrate binding, water 389 would not be available to accept a proton from the C2 hydroxyl group, as described below in the proposed ring opening mechanism. It is only after the conformational change in the substrate and the loss of water 389 that the helix containing residues 513−520 can move in toward the substrate. In contrast to the model we presented previously based on only the PGI/6PGA and PGI/5PAA structures (*19*), in our new model it is only after the ring opening step that the helix containing amino acids 513−520 moves; this shift is not concurrent with substrate binding.

Mechanism of Reaction. Extensive biochemical characterization of PGI has led to a proposed multistep reaction mechanism that involves general acid/base catalysis with proton transfer. In the forward reaction, the cyclic form of G6P binds to the active site, and the enzyme first catalyzes ring opening to yield the open chain form of G6P. The ring opening step is followed by an isomerization step involving proton transfer between C2 and C1 that yields the open chain form of the product, F6P. In the reverse reaction, the enzyme catalyzes ring opening of F6P, and proton transfer proceeds from C1 to C2 to yield G6P.

Analysis of a previously reported rabbit PGI/5PAA structure identified Glu357 as a candidate for the residue that transfers a proton between C1 and C2 of the intermediate during catalysis, and Arg272 was proposed to be involved in stabilization of the 1,2-*cis*-enediol(ate) intermediate (*19*). However, none of the previously reported structures identified the residues involved in the ring opening step. The new structure with F6P bound in its cyclic form enables us to identify the residues that are in positions where they could

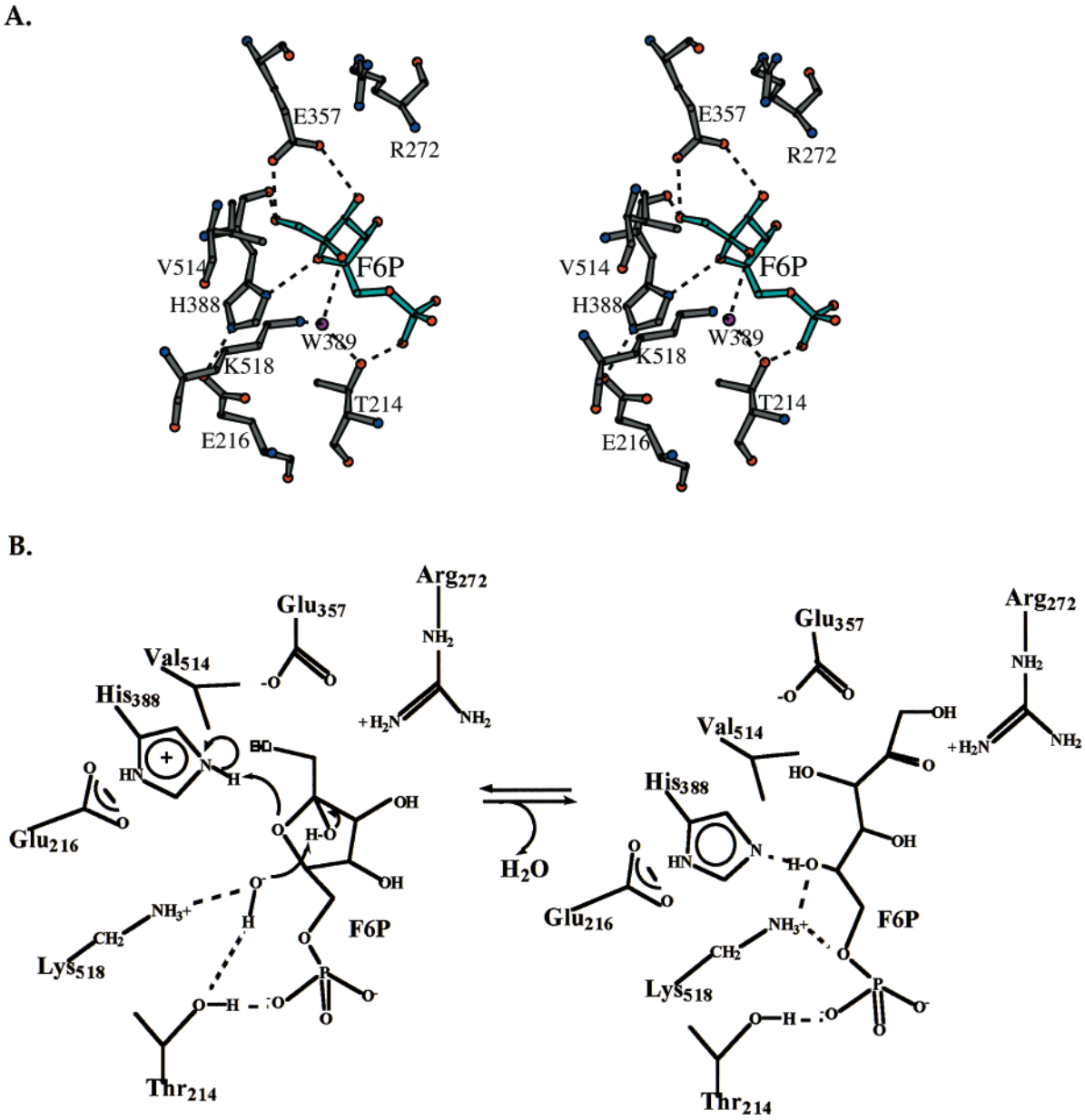

FIGURE 3: Proposed mechanism for the ring opening step. (A) Stereo diagram of the PGI active site indicating key interactions in the ring opening step. Hydrogen bonds between the cyclic form of F6P and active site amino acid residues His388, Lys518, and Thr214 and water 389 are shown as dashed lines. (B) Schematic diagram of the mechanism of the proposed ring opening step and subsequent conformational changes. His388 protonates the ring oxygen of D-fructose 6-phosphate to catalyze the ring opening step and yield the open chain form of D-fructose 6-phosphate. Water 389 accepts the proton from the C2 hydroxyl group. Removal of water 389 and a conformational change in the substrate allow the helix-containing amino acid residues Lys518 and Val514 to move closer to the substrate. In its new conformation, the substrate C1 and C2 are closer to Glu357 and Arg272, which have previously been proposed to be involved in the isomerization step.

catalyze ring opening. In the new PGI/F6P complex structure, His388 and Lys518 are the closest amino acids to the F6P ring oxygen and the hydroxyl group on C2 (Figure 3A). The side chain nitrogen (Nδ1) of His388 is 2.9 Å from the F6P ring oxygen. Glu216 helps to position the side chain of His388. The ϵ nitrogen of Lys518 is 4.2 Å from OH2. Water 389 is located between the ϵ nitrogen of Lys518 and the C2 hydroxyl group of the substrate (2.7 and 2.2 Å, respectively). Water 389 also forms a hydrogen bond with the side chain hydroxyl group of Thr214.

On the basis of the PGI/F6P complex crystal structure, we propose the following mechanism for the ring opening step (Figure 3B): After the cyclic form of F6P binds to the PGI active site, protonation of the ring oxygen by His388 provides a driving force that promotes an electron shift resulting in opening of the hexose ring. During the ring opening step, the proton on the hydroxyl group at C2 must be removed. It could possibly be transferred to the bulk solvent, but it is more likely transferred to water 389. The hydroxyl group on Thr214 also interacts with one of the negatively charged oxygens on the substrate phosphoryl group, and the proton on the Thr214 hydroxyl group will be located between the Thr214 side chain oxygen and the phosphate oxygen. A lone pair of electrons on the Thr214 side chain oxygen will be oriented toward water 389, so one proton of water 389 will be located between the water 389 oxygen and the Thr214 side chain oxygen. The lone pairs of water 389 will be oriented toward the substrate C2

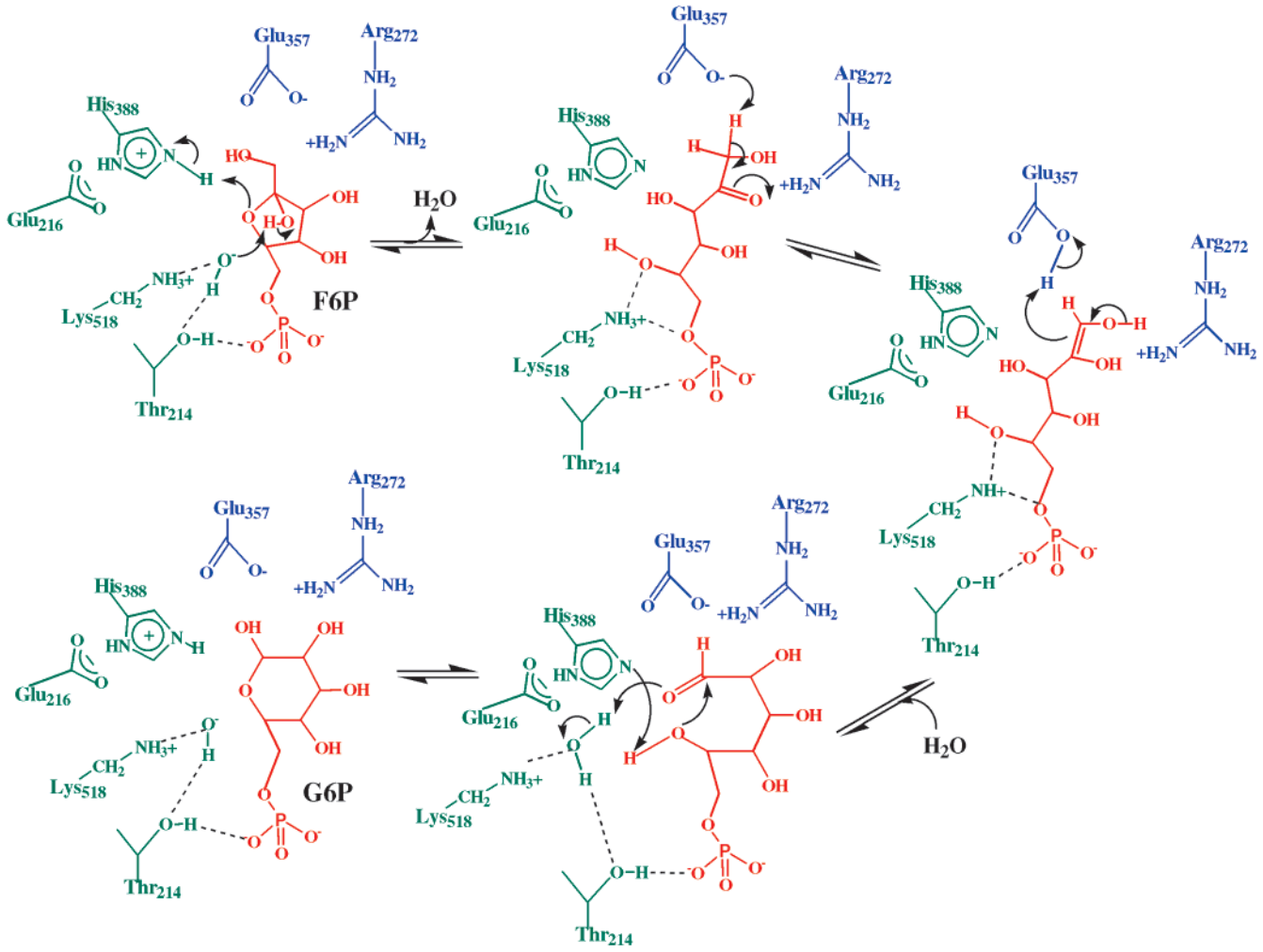

FIGURE 4: Proposed roles for active site amino acid residues in the multistep catalytic mechanism for phosphoglucose isomerase. A schematic diagram of the ring opening, isomerization, and ring closing steps is shown. The substrate and intermediates are shown in red. Amino acids involved in the ring opening step are shown in green, and amino acids involved in the isomerization step are shown in blue. The ring closing step is proposed to be the reverse of the ring opening step, except that a bond is formed between O5 and C1 instead of C2.

hydroxyl group and the side chain of Lys518. Water 389 can thus accept the proton from O2 to become a hydronium ion. Alternatively, water 389 could be a hydroxide anion that is stabilized by hydrogen bonding to Lys518, Thr214, and the C2 hydroxyl group (Figure 3B). After accepting a proton from the substrate, the resulting hydronium ion or water molecule would be lost to solvent. The removal of water 389 is important for the protein conformational change that follows the ring opening step.

The ring opening mechanism is also included in a schematic diagram of our proposed PGI multistep catalytic mechanism (Figure 4). After the ring opening step and conformational changes in the protein and substrate as described above, the isomerization step can proceed as previously proposed: Glu357 abstracts a proton from C1 of the substrate, and electron shifts result in the formation of a double bond between C1 and C2, yielding the *cis*-enediol(ate) intermediate. Glu357 then transfers the same proton back to the *cis*-enediol(ate) intermediate at C2. The cyclic form of G6P can then be formed by a reversal of the ring opening step, except that a bond is formed between O5 and C1 instead of C2. A water molecule from the solvent would bind between Lys518 and the substrate and donate a proton to the substrate aldehyde oxygen, and His388 would accept the proton from the C5 hydroxyl group.

This mechanism is consistent with previously reported biochemical characterization of the enzyme, including pH profile and chemical modification experiments. The results of pH profile experiments suggested functional groups with pK_a's of 6.7 and 9.4, possibly a histidine and a lysine, are involved in catalysis (*13*, *26*, *27*). The results of chemical modification studies have suggested that histidine (*28*), lysine (*29*), and glutamate (*30*) residues are involved in the reaction. In addition, His388, Lys518, and Glu357 were found to be strictly conserved in 127 phosphoglucose isomerase sequences (*19*).

CONCLUSIONS

A 2.1 Å resolution structure of PGI complexed with bound fructose 6-phosphate substrate has been determined. The fructose 6-phosphate substrate is found bound to the active site in its cyclic form, and consistent with previously reported structures of rabbit PGI with bound 6PGA or 5PAA, it is oriented so that its phosphate group interacts with Thr211, Thr214, Ser159, Ser209, and Lys210. The structure with bound F6P predicts that His388 catalyzes the ring opening

step of the proposed multistep catalytic mechanism. Comparison with the previously reported PGI/5PAA structure indicates that the helix containing residues 513−520 moves in toward the substrate after the ring opening step and before the isomerization step. This movement is made possible by the loss of water 389 and a conformational change in the substrate.

ACKNOWLEDGMENT

We thank the BioCars staff for support and assistance in data collection at APS Sector 14 at Argonne National Laboratories.

REFERENCES

1. Chaput, M., Claes, V., Portetelle, D., Cludts, I., Cravador, A., Burny, A., Gras, H., and Tartar, A. (1988) *Nature 332*, 454−455.
2. Faik, P., Walker, J. I., Redmill, A. A., and Morgan, M. J. (1988) *Nature 332*, 455−457.
3. Watanabe, H., Takehana, K., Date, M., Shinozaki, T., and Raz, A. (1996) *Cancer Res. 56*, 2960−2963.
4. Niinaka, Y., Paku, S., Haga, A., Watanabe, H., and Raz, A. (1998) *Cancer Res. 58*, 2667−2674.
5. Xu, W., Seiter, K., Feldman, E., Ahmed, T., and Chiao, J. W. (1996) *Blood 87*, 4502−4506.
6. Gurney, M. E., Apatoff, B. R., Spear, G. T., Baumel, M. J., Antel, J. P., Bania, M. B., and Reder, A. T. (1986) *Science 234*, 574−581.
7. Gurney, M. E., Heinrich, S. P., Lee, M. R., and Yin, H. S. (1986) *Science 234*, 566−574.
8. Chiao, J. W., Zu, W., Seiter, K., Feldman, E., and Ahmed, T. (1999) *Leuk. Res. 23*, 13−18.
9. Abolhassani, M., Riley, W. M., Feldman, E., Arlin, Z., and Chiao, J. W. (1990) *Proc. Soc. Exp. Biol. Med. 195*, 288−291.
10. Leung, K., and Chiao, J. W. (1985) *Proc. Natl. Acad. Sci. U.S.A. 82*, 1209−1213.
11. Lohmann, K. (1933) *Biochem. Z. 262*, 137.
12. Rose, I. A., and O'Connell, E. L. (1961) *J. Biol. Chem. 236*, 3086−3092.
13. Rose, I. A. (1975) *Adv. Enzymol. Relat. Areas Mol. Biol. 43*, 491−517.
14. Rose, I. A. (1981) *Philos. Trans. R. Soc. London, Ser. B 293*, 131−143.
15. Willem, R., Malaisse-Lagae, F., Ottinger, R., and Malaisse, W. J. (1990) *Biochem. J. 265*, 519−524.
16. Swenson, C. A., and Barker, R. (1971) *Biochemistry 10*, 3151−3154.
17. Schray, K. J., Benkovic, S. J., Benkovic, P. A., and Rose, I. A. (1973) *J. Biol. Chem. 248*, 2219−2224.
18. Jeffery, C. J., Bahnson, B. J., Chien, W., Ringe, D., and Petsko, G. A. (2000) *Biochemistry 39*, 955−964.
19. Jeffery, C. J., Hardré, R., and Salmon, L. (2001) *Biochemistry* (in press).
20. Chou, C. C., Sun, Y. J., Meng, M., and Hsiao, C. D. (2000) *J. Biol. Chem. 275*, 23154−23160.
21. Otwinowski, Z., and Minor, W. (1997) in Processing of X-ray diffraction data collected in oscillation mode, in *Macromolecular Crystallography, Part A* (Carter, C. W., Ed.) pp 307−326, Academic Press, New York.
22. Brunger, A. T., Adams, P. D., Clore, G. M., DeLano, W. L., Gros, P., Grosse-Kunstleve, R. W., Jiang, J. S., Kuszewski, J., Nilges, M., Pannu, N. S., Read, R. J., Rice, L. M., Simonson, T., and Warren, G. L. (1998) *Acta Crystallogr. D54*, 905−921.
23. Jones, T. A., Zou, J. Y., Cowan, S. W., and Kjeldgaard, M. (1991) *Acta Crystallogr. A47*, 110−119.
24. Brunger, A. T. (1992) *Nature 355*, 472−474.
25. Collaborative Computational Project, No. 4 (1994) *Acta Crystallogr. D50*, 760−763.
26. Dyson, J. E., and Noltmann, E. A. (1968) *J. Biol. Chem. 243*, 1401−1414.
27. Hines, M. C., and Wolfe, R. C. (1963) *Biochemistry 2*, 770−775.
28. Gibson, D. R., Gracy, R. W., and Hartman, F. C. (1980) *J. Biol. Chem. 255*, 9369−9374.
29. Schnackerz, K. D., and Noltmann, E. A. (1971) *Biochemistry 10*, 4837−4843.
30. O'Connell, E. L., and Rose, I. A. (1973) *J. Biol. Chem. 248*, 2225−2231.
31. Esnouf, R. M. (1997) *J. Mol. Graphics 15*, 133−138.

BI002916O